From the source to the reservoir and beyond - tracking sediment particles with modeling tools under climate change predictions (Carpathian Mts.)

Paweł Wilk[1*], Monika Szlapa[2], Paweł S. Hachaj[2], Paulina Orlińska-Woźniak[1], Ewa Jakusik[1], Ewa Szalińska[3]

[1] Institute of Meteorology and Water Management, National Research Institute, Podleśna 61, 01-673 Warsaw, Poland

[2] Faculty of Environmental and Power Engineering, Cracow University of Technology, Warszawska 24, 31-155 Cracow, Poland

[3] Faculty of Geology, Geophysics and Environmental Protection, AGH University of Science and Technology, A. Mickiewicza Av. 30, 30-059 Cracow, Poland

[*] Corresponding Author: pawel.wilk@imgw.pl, https://orcid.org/0000-0003-4302-5059

Key points

- Combined SWAT and AdH/PTM models have been used to track the sediment fractions delivered from the Carpathian catchment to the drinking water reservoir.
- Loads of the mineral fractions are expected to increase significantly during high flow months as a result of climate change.
- Increased mobility of fine particles in the reservoir can be a risk due to their role as contaminant carriers.

Keywords sediment fractions, river, dammed reservoir, Macromodel DNS/SWAT, AdH/PTM,

Abstract Transport of sediment particles from the source of their origin to a deposition area is of utmost importance, especially in catchments very prone to erosion. Especially, since future climate changes are predicted to enhance severity of the sediment transport issues, particularly in catchments with dammed reservoirs, which capacity and water quality can be extremely altered. In the current study we tracked, with a monthly step, two mineral and one mineral/organic sediment fraction delivered from the Carpathian Mts. catchment (Raba River) to the drinking water reservoir (Dobczyce). This was possible by combining SWAT and AdH/PTM models on the digital platform - Macromodel DNS. Moreover, we have applied a variant scenario analysis including RCP 4.5 and 8.5, and land use change forecasts. The results highlighted the differences between the two analyzed hydrological units and showed large variability of the

sediment load between months. The predicted climate changes will cause a significant increase of mineral fraction loads (silt and clay) during months with high flows. Due to the location and natural arrangement of the reservoir, silt particles will mainly affect faster loss of the first two reservoir zones capacities, which is consistent with their intended use as traps for larger fractions. The increased mobility of the finer particles (clay) in the reservoir may be more problematic in the future. Mainly due to their binding pollutant properties, and the possible negative impact on drinking water abstraction from the last reservoir zone.

Introduction

Natural processes, such as erosion, sediment transport and its deposition can shape the land surface, and influence the structure and function of river catchment ecosystems worldwide [Guillén Ludeña et al., 2017; Vercruysse et al., 2017; Wu et al., 2018; Stähly et al., 2020; Hu et al., 2021; Feng and Shen., 2021]. However, these processes are very sensitive to both climate change and land use, especially in mountainous areas [Hohmann et al., 2018; Dibike et al., 2018; Zhao et al., 2018; Aksoy et al., 2019; Zhang et al., 2020]. Already, many mountain catchments are struggling with an increase in soil loss due to intensification of rainfall, and consequently, surface runoff [Halecki et al., 2018a-b; Borrelli et al., 2018; Mostowik et al., 2019; Berteni and Grossi, 2020; Ciampalini et al., 2020]. Moreover, the forecasted changes in precipitation and temperature suggest that an intensity of this phenomenon may increase significantly [Borrelli et al., 2020; Gianinetto et al., 2020; Szalińska et al., 2020]. It also turns out that in such areas even favorable changes in land use (LU), associated with a significant increase in the area of forests, naturally stabilizing the soil, may turn out to be insufficient to stop the negative effects of the climate changes [Orlińska-Woźniak et al., 2020a].

The consequences will be particularly severe in catchments with dammed reservoirs, trapping most of the sediment particles. Sediment entrapment has long been a major factor in reducing the capacity and deterioration of water quality in many reservoirs around the world, endangering their durability, human health, and safety [Zarfl and Lucía, 2018; Bilali et al., 2020; Huang et al., 2021]. Multiple studies have shown today, as a result of the increase in sediment loads transported by rivers into reservoirs, that each year about 1% of their total capacity in the world is lost [Antoine et al., 2020]. In order to effectively stop, or at least mitigate this negative trend, it is necessary to precisely predict the effects of climate and land use changes in river catchment systems. Environmental models can play a key role in this, and research with their use has been conducted for many years, allowing i.e., to estimate sediment loads introduced

into the reservoir, the effectiveness of the reservoir as a sediment trap, loss of reservoir volume, and finally to identify areas of sediment deposition [Croley et al. 1978; Banasik et al. 1993; Garg and Jothiprakash 2010; Wisser et al. 2013; Charafi 2019; Bladé Castellet 2019]. Unfortunately, they very often do not take into account important elements such as the fate of individual grain fractions, the movement of sediments downstream from the reservoir, or more, the role of reservoir backwater. The river and the reservoir form two separate entities in terms of hydrology, with a complex and stochastic nature of the processes of transport, and deposition of sediment particles [Idrees et al., 2021]. As a result, integration attempts in the river and dam reservoir model are still rare, making it difficult to keep track of the sediments during simulation.

We attempted to face this challenge by using the capabilities of the digital platform - Macromodel DNS [Wilk et al., 2018a; Orlińska-Woźniak et al., 2020a; Szalińska et al., 2021], allowing for integration of two advanced environmental models (SWAT and AdH/PTM) [Arnold et al., 2012; Burgan et al., 2019; MacDonald et al., 2006]. For the first time, these tools were combined as modules on the platform, thus obtaining a unique ability to precisely track sediment particles of individual fractions from their source, through transport, and ultimately to their deposition in a designated reservoir zone [Kimmel et al. 1990; Thornton et al. 1996; Green et al, 2015]. Moreover, the conducted analyzes included four detailed variant scenarios which took into account both monthly changes of climate (precipitation and temperature) in short- and long-time horizons, as well as changes in land use (forest and urban areas). This enabled the precise indication of critical periods for the sediment load increase in the reservoir. The developed tool was used for the mountain catchment of the upper Raba River, located in the Polish part of the Carpathian Mountains, and flowing into the Dobczyce Reservoir. This area is distinguished by intensity of meteorological phenomena and water erosion [Miluś et al., 2019; Orlińska-Woźniak et al., 2020a; Szalińska et al., 2020]. Moreover, land use forecasts indicate a gradual increase in forest cover in this area [Kozak et al., 2017; Price et al. 2017]. The reservoir itself is the main source of drinking water for one of the largest agglomerations in Poland, and serves as flood protection. Ultimately, it was possible to track two mineral (SILT, CLAY) and one organic-mineral fraction (SMAG), taking into account the different nature of the catchment area and reservoir, and their different sensitivities to future changes. As a consequence, we were able to show the effects of the implementation in the variant scenario model, both for the catchment area, and subsequent zones of the dammed reservoir in a monthly time step.

Data and Methods

2.1 Study area

The study area consists of two parts, the upper Raba River catchment (RR), and the Dobczyce Reservoir (DR) (Figure 1). The upper Raba River flows 60 km from its source, located in the Carpathian Gorce Mts. (780 m a.s.l.), to the Dobczyce dammed reservoir (265 m a.s.l.). The RR catchment covers an area of 768 km^2 [Mazurkiewicz-Boroń 2016; Operacz 2017; Mikuś et al., 2019], and has a typically mountainous character with almost 43% of the area covered by slopes over 25%, and overgrown by forest (Figure 2). The mountainous nature of this catchment also manifests with a fast reaction to precipitation. The river features very large amplitudes of water levels and flows, with maximum values recorded in the snow melt period, and early-summer long-lasting rainfall events. The studied catchment is covered generally by clays, and its lower slopes are used mostly for agricultural activities (over 40%). The entire area is well known as being particularly vulnerable to water erosion [Partyka, 2002; Kijowska-Strugała et al., 2017; Halecki et al., 2018].

The Dobczyce Reservoir was created as a result of dam construction (1986) undertaken to provide drinking water supplies for approx. half a million people, and to regulate the river flows [Mazurkiewicz-Boron 2016; Hachaj, 2019]. It is a multipurpose dam reservoir supplying people with drinking water, protecting against floods and droughts, producing electricity, and being a place for fish farming. The created reservoir has an area of approx. 10.7 km^2 (length of 8 km and width of 1.6 km), and an average depth of 12 m (maximum of 35 m) [Hachaj and Szlapa, 2017; Zemełka et al., 2019; Wilk-Woźniak et al., 2021]. The reservoir is divided into four zones (Figure 3) including a riverine part (A), backwater (B), Myślenice basin (C), and Dobczyce basin (D) closed by the dam cross-section (OUT). The entire area of the upper Raba River catchment belongs to the Carpathian climatic region of Poland [Kędra and Szczepanek, 2019; Hachaj and Kołodziejczyk 2020] where the topography has a great influence on climatic conditions [Wypych et al., 2017; Wypych et al., 2018]. Average annual air temperature is around 7°C, however, the annual temperature amplitude reaches 21°C. The average rainfall ranges from about 700 mm to about 1600 mm at the higher altitudes [Gorczyca et al., 2018]. The growing season lasts about 200-210 days (April to mid-October).

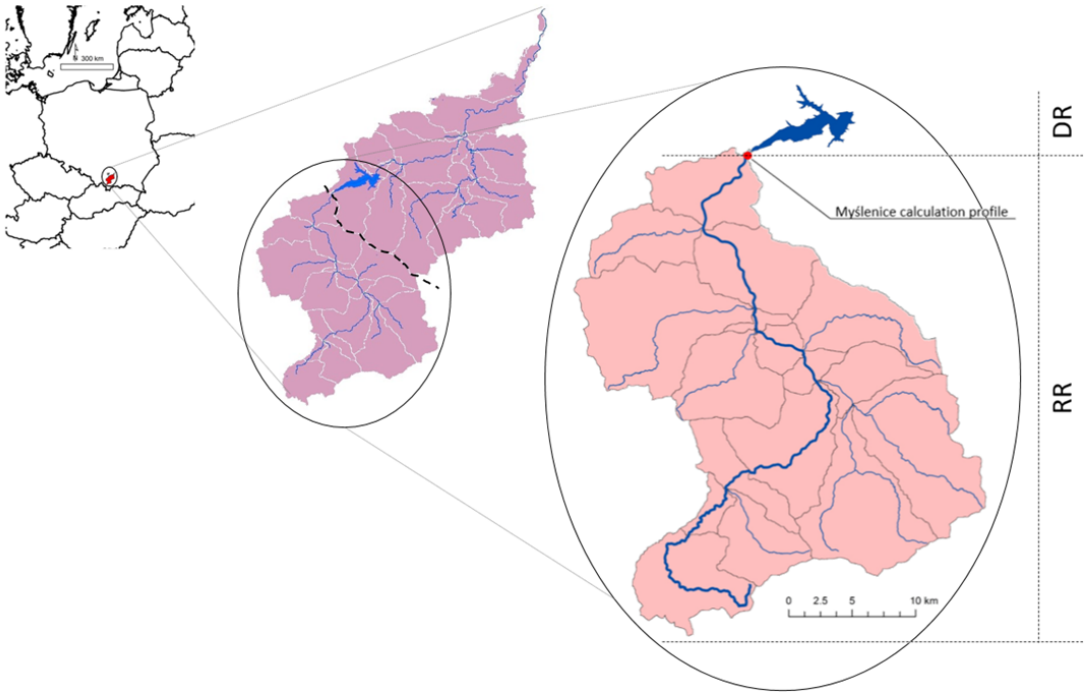

Figure 1. The research area with division into the upper Raba River catchment (RR), and the Dobczyce Reservoir (DR).

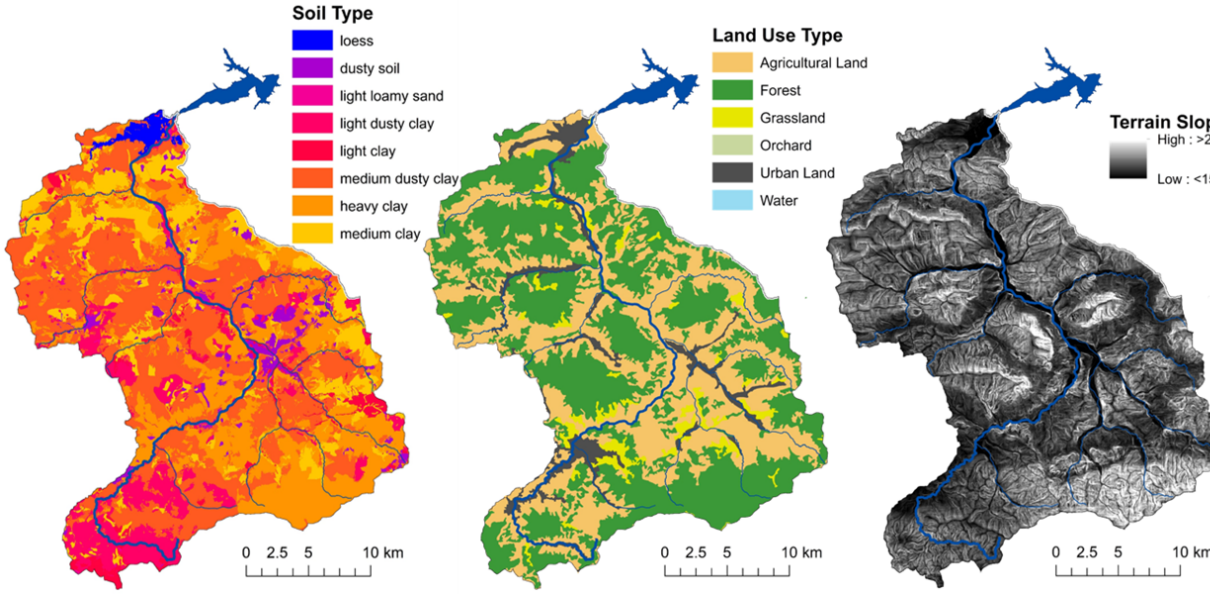

Figure 2. The upper Raba River catchment (RR) with soil, land use

type, and terrain slopes.

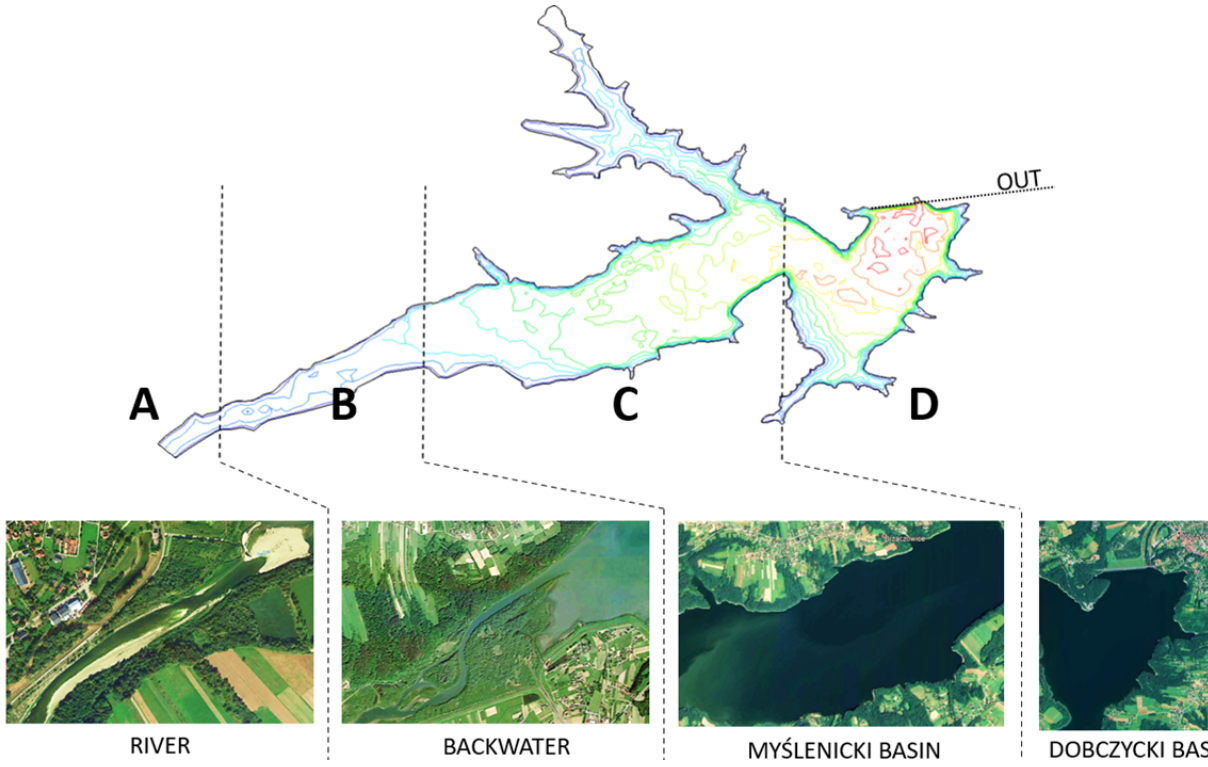

Figure 3. Division of the Dobczyce Reservoir (DR) into four zones [source: Google Maps].

2.2 Modeling tool

To achieve the goal of the study, i.e., to track sediment particles from their source to the deposition area, the DNS (Discharge-Nutrient-Sea) digital platform (Macromodel DNS) has been used as a modeling tool. The Macromodel DNS, developed at the Institute of Meteorology and Water Management - National Research Institute [Wilk et al., 2018b; Wilk and Orlińska-Woźniak, 2019], provides an interactive platform allowing for integration of the SWAT (Soil and Water Assessment Tool) module (version 2012) [Arnold et al., 2012; Abbaspour et al. 2015] with other modeling tools (modules) to track different processes of the sediment/contaminant transport in a catchment [Wilk et al., 2018a; Szalińska et al., 2020; Orlińska-Woźniak et al., 2020a; Szalińska et al., 2021]. The RR catchment module has been created in the SWAT module (Figure 4) with use of the following data:

- map of Poland hydrographical divisions, scale of 1:10,000 (source: IMGW-

PIB, resolution: 5 m);

- digital elevation model (DEM), scale of 1:20,000 (source: IMGW-PIB, resolution: 10 m);
- land use map - based on Corine Land Cover (CLC 2012), and agrotechnical data from the Local Data Bank (Figure 2b) (source: Copernicus Programme, resolution 20 m);
- soil map - detailed data on soil types, scale of 1:5,000 (Figure 2c) (source: Institute of Soil Science and Plant Cultivation, resolution 2.5 m);
- meteorological data (1992–2016, e.g., precipitation and temperature) for 75 stations located directly in the catchment, and within 20 km from its borders (source: IMGW-PIB).

Subsequently, the created RR module has been used to simulate sediment yields from the catchment (land phase) and sediment loads (river phase) delivered to the reservoir (DR). Moreover, the SWAT module has been also used to estimate the sediment loads discharged into the DR in future time horizons under climate and land use changes.

To simulate sediment transport and deposition processes into the DR, two additional modules have been incorporated into the DNS digital platform. Hydraulic conditions in the DR for sediment load scenarios have been modeled with use of the AdH (Adaptive Hydraulics Model) module, while the particle transport within the DR has been simulated with the use of the PTM (Particle Tracking Model) module (Figure 4) [Burgan and Icaga, 2019; Jiang et al., 2021]. The DR module has been created with use of the following data:

- numerical model of the Dobczyce Reservoir bottom from the Cracow University of Technology, Faculty of Environmental and Power Engineering (CUT FEPE) own data of the DR bottom shape;
- backwater shape updated based on the IMGW-PIB bathymetry map from 2008, scale of 1:10,000.

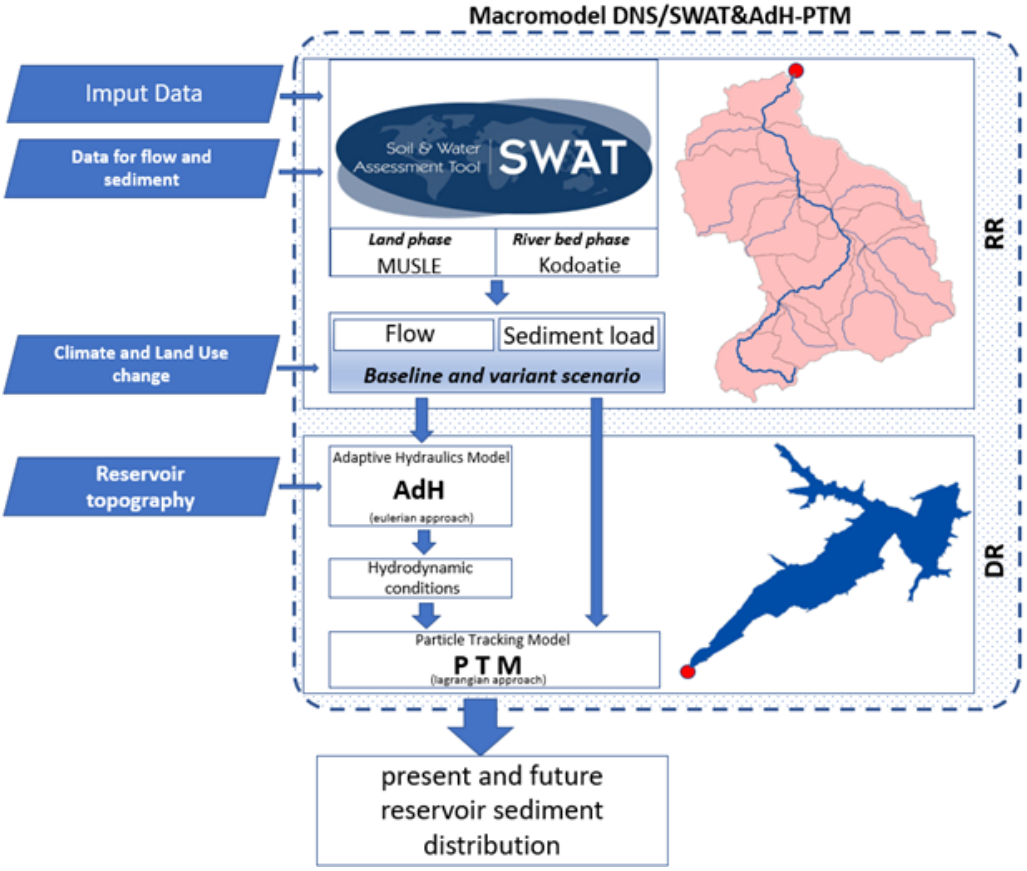

Figure 4. Modeling flow-chart.

2.2.1 SWAT module

The module of the RR applied in the current study catchment has been adopted from the model built for the entire Raba River catchment area, calibrated and validated for flow and sediment as described previously [Szalińska et al., 2020; Orlińska-Woźniak et al., 2020a]. The upper part of the catchment (Figure 1) has been separated using the GIS tool and the catchment boundaries, respective to the Myślenice calculation profile, located directly upstream from the DR. The land phase of the model (sediment yields) has been simulated for all RR 17 sub-catchments, delineated as hydrological response units (HRUs) combining unique land use, soil type, and slope features. The sediment yield estimations (SYLD) have been based on the Modified Universal Soil Loss Equation (MUSLE), embedded in the SWAT module, according to Eq. (1) [Williams, 1975; Vigiak et al., 2015]:

$sed = 11.8 * (Q_{\text{surf}} * q_{\text{peak}} * \text{area}_{\text{HRU}})^{0.56} * K_{\text{USLE}} * C_{\text{USLE}} * P_{\text{USLE}} * \text{LS}_{\text{USLE}} * CFRG$ (1)

where: *sed* is the sediment yield on a given day (metric tons), Q_{surf} is the surface runoff volume (mmH2O/ha), q_{peak} is the peak runof rate (m3/s), *area HRU* is the area of the HRU (ha), K_{USLE} is the USLE soil erodibility factor (0.013 metric ton m2hr/(m3-metric ton cm)), C_{USLE} is the USLE cover and management factor, P_{USLE} is the USLE support practice factor, LS_{USLE} is the USLE topographic factor, and *CFRG* is the coarse fragment factor.

To simulate the river bed phase of the sediment transport, the Kodoatie method [Kodoatie 2000] also available in the SWAT module, has been used according to Eq. (2).

$\text{conc}_{sed,ch,mx} = \left(\frac{a*v_{\text{ch}}^{b}*y*S^{d}}{Q_{\text{in}}}\right) * \left(\frac{W+W_{\text{btm}}}{2}\right)$ (2)

where: $\text{conc}_{sed,ch,mx}$ is the maximum sediment concentration (t m−3); v_{ch}^{b} is mean flow velocity (m s−1); y is mean flow depth (m); S is energy slope (m m−1); Q_{in} is water entering the reach (m3); *a, b, c,* and *d* are regression coefficients for different bed materials; *W* is channel width at the water level (m), and W_{btm} is bottom width of the channel (m).

This method is considered to be particularly effective for suspended and small sediment particles [Simons et al., 2004; Neitsch et al., 2011, Yen et al., 2017]. Therefore, the sediment loads for the Myślenice calculation profile has been estimated for the following fractions (mineral: CLAY - 0-0.004 mm, SILT - 0.004-0.062 mm, and mineral/organic: SMAG - 0.03 mm) [Lu et al., 2015; Ayaseh et al., 2019; Orlińska-Woźniak et al., 2020a].

The climate change predictions were based on data from Euro-CORDEX, RCM models [Rummukainen, 2016; Dosio, 2016], and Global Climate Models - GCM [Yang et al., 2019]. They included RCP4.5 and RCP8.5 emission scenarios for the short-term (H1, average for 2026-2035) and long-term (H2, average for 2046-2055) time horizons. The scenarios employed to estimate sediment load discharged into the DR were adopted from the Polish Development of Urban Adaptation Plans (UAP) [MPA, 2021a; MPA, 2021b], which have been described in detail in previous studies [Orlińska-Woźniak et al., 2020b; Szalińska et al., 2021]. Briefly, besides the baseline scenario, four climate scenarios (VS1-VS4) have been created covering predicted temperature and precipitation changes under the short-term (H1) and long term (H2) perspective (Figure 5a) as follows:

- VS1 - RCP4.5 H1 - average for 2026-2035;

- VS2 - RCP4.5 H2 - average for 2046-2055;
- VS3 - RCP8.5 H1 - average for 2026-2035;
- VS4 - RCP8.5 H2 - average for 2046-2055.

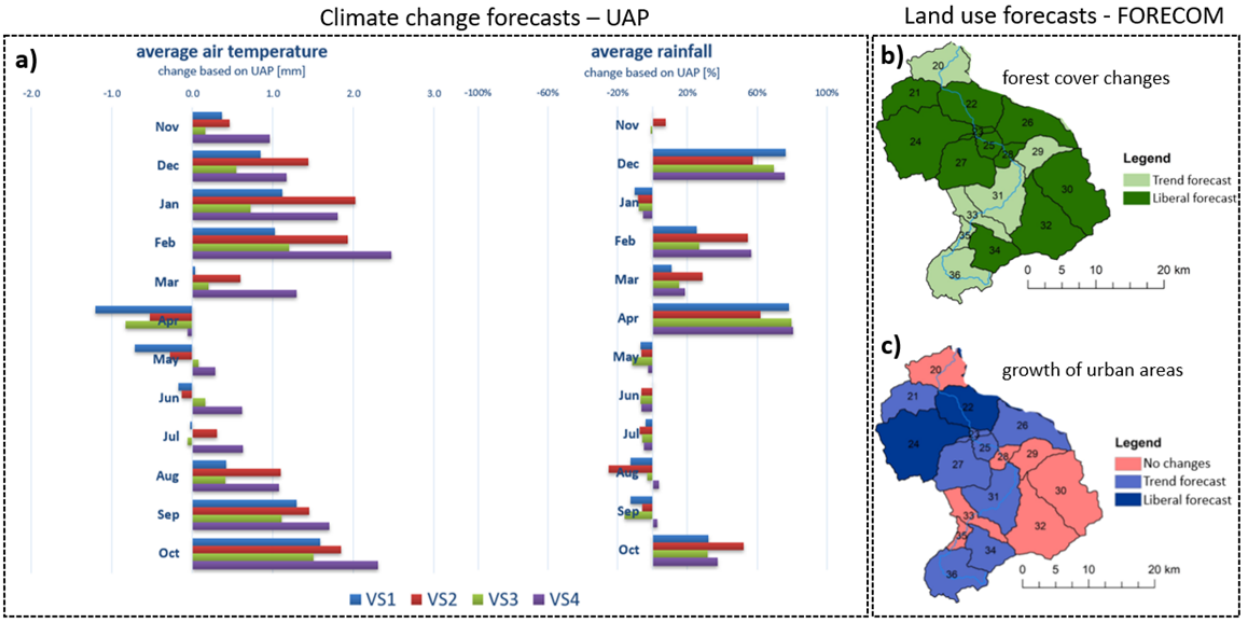

Figure 5. Forecasted changes in climate: temperature and precipitation (a); together with forecasts of changes in LU of forest areas (b), and urbanized areas (c).

Along with the climate change predictions, the LU future changes have also been taken into consideration, and were included in each VS since they occur concurrently. The estimate projected on LU change impacts on sediment loads in the RR were based on results of the FORECOM project (http://www.gis.geo.uj.edu.pl/FORECOM/index.html), and transposed into the analyzed area with use of the DYNA-Clue model for the future time horizon of 2060 [Kozak et al., 2017; Price et al. 2017]. Briefly, LU scenarios included future changes in the forest cover and growth of urban areas (based on population density). Depending on the scenario, one of the following forecasts was assigned to each RR sub-catchment: trend (growth of forest and urban areas by 23% and 10%, respectively), or liberal (growth of forest and urban areas, respectively by 30% and 15%) (Figure 5b-c) [Orlińska-Woźniak et al., 2020a].

2.2.2 AdH/PTM module

To execute the sediment transport and deposition simulations in the DR, previously built and validated data using the comparative analysis with the real AdH/PTM model data [Hachaj and Szlapa, 2017; Hachaj, 2018; Hachaj, 2019], was adapted in the current study. AdH is a 2D depth-averaged finite element hydrodynamic modeling tool for simulating estuary water flow and hydrodynamics in reservoirs and lakes. It uses the finite element method to solve two-dimensional momentum conservation equations for water - in the Eulerian frame for both x and y directions [Berger, 2010] according to Eq. (3):

$$\begin{cases} \frac{\partial v_x}{\partial t} + v_x \frac{\partial v_x}{\partial x} + v_y \frac{\partial v_x}{\partial y} * \ C_f * v_y + g \frac{\partial \zeta}{\partial x} + g * v_x \frac{\sqrt{v_x^2 + v_y^2}}{C^2 * H} * v \left(\frac{\partial^2 v_x}{\partial x^2} + \frac{\partial^2 v_x}{\partial y^2} \right) + \frac{1}{\rho_w} \frac{\partial p}{\partial x} = f_x \\ \frac{\partial v_y}{\partial t} + v_x \frac{\partial v_y}{\partial x} + v_y \frac{\partial v_y}{\partial y} * C_f * v_x + g \frac{\partial \zeta}{\partial y} + g * v_y \frac{\sqrt{v_x^2 + v_y^2}}{C^2 * H} * v \left(\frac{\partial^2 v_x}{\partial x^2} + \frac{\partial^2 v_x}{\partial y^2} \right) + \frac{1}{\rho_w} \frac{\partial p}{\partial x} = f_y \end{cases}, \quad (3)$$

where: vx, vy – velocity components in x and y directions, respectively [m/s]; fx [m/s2] – unitary force in the x direction, represented by wind-induced surface friction, wave impact; fy [m/s2] – unitary force (wind, waves…) in the y direction; Cf [1/s] – Coriolis factor; g [m/s2] – gravitational acceleration, " " [m] – water surface elevation, H [m] – depth, C [m1/2/s] – Chezy roughness coefficient, [m2/s] kinematic viscosity coefficient, and p [Pa] – external pressure.

In the current approach, the boundary conditions of the DR AdH model, i.e., inflow rate and water surface elevation level (WSE), were adapted to include monthly Average High Flow (AHQ) and normal water surface level - 269.9 m a.s.l. The simulation was performed with the default bottom roughness parameter, and water density, as well as the neglected impact of wind, wave, and Coriolis forces. The AHQ values [Wrzesiński and Sobkowiak, 2020; Luong et al., 2021] were calculated using flow data simulated by the SWAT module for each VS according to Eq. (4):

$$\mathrm{AHQ}_m = \frac{\sum_{i=1}^{y} \max_{m,y}(Qd)}{Y} \quad (4)$$

where: AHQ - average high flow for a given month, Y - number of years within the data series, and max(Q_d) - the highest daily flow observed within a calendar month (m index of AHQ and the max operator) of a given year (y index of the max operator).

Based on the planar velocity field calculated by the AdH module, the particle's behavior over time (entrainment, advection, diffusion, settling, deposition, burying, etc.) the DR was simulated with the PTM module. At each time-step, PTM performs calculations to determine local characteristics of the environment (Euler frame, mesh-based), and the behavior of each tracked representative particle (Lagrange

frame, particle-based). The potential transport rate of sediment particles was calculated by the Soulsby-van Rijn method based on Eq. (5), while the other equations used by PTM, including the calculation of the particle trajectory is presented in [Niel, 2006].

$$q_t = A_s \overline{U} \left(\left(\overline{U}^2 + \frac{0.018}{C_D} \overline{U_w}^2 \right)^{\frac{1}{2}} - U_{\mathrm{cr}} \right)^{2.4} \quad (5)$$

where: qt – total transport rate; As – coefficient dependent on grain size; U – depth-averaged planar velocity; Uw – average wave orbital velocity; CD – wave drag coefficient; and Ucr – critical (threshold) velocity for motion/suspension regimes U.

The calculation profile of Myślenice, previously used as the closure of the RR part in the SWAT module, was selected as the source of the sediment for the PTM simulation in the DR part. To ensure that all the model-generated representative particles will start their movement in the water, the source area was set as an ellipsoid with the center point on 1.9 m above the bed and with the vertical and horizontal radii of 1 and 25 m, respectively. These dimensions were determined by the shape of the river bed in the place where the sediment source is located and allowed for the maximum filling of the selected profile with the shape of an ellipsoid. Simulations were performed using sediment density of 2650 kg/m3 and 1240 kg/m3 for mineral particles and mineral/organic aggregates, respectively [Czuba et al., 2015]. As for the particle diameter the following values have been adopted: CLAY d= 0.002mm (dev=1.25), SILT d=0.05mm (dev=1.2), SMAG d=0.03 mm (no deviation). In order to ensure better visualization possibilities, the number of generated representative particles of each of the three different kinds was chosen to be roughly proportional to the appropriate mass loads calculated by the SWAT module for a given month. Differences from exact proportions are the effect of randomization. Note, that for all the analyses shown below, the exact number of generated representative particles has negligible impact on the results. This is because the analyses use only a fraction comparison (e.g., what percentage of the total number of particles is deposited in a given catchment in a given month), which does not depend on the size of the random sample as long as the sample is large enough.

Results

3.1. The upper Raba River (RR) simulations

3.1.1. Sediment loads

The average sediment monthly loads (tons per month - t/m) for

the Myślenice calculation profile produced with use of the SWAT module have been presented in Table 1. For all the three analyzed sediment fractions (SMAG, SILT, and CLAY) high variability of loads is clearly visible with the coefficient of variation (CV) ranging from 85 to 191%. Following monthly distribution, two periods can be distinguished, one from October till April, and the second one from May to September. During the first one, average loads reached about 6 t/m for the SILT fraction, and 220 t/m for CLAY. While the loads for SMAG were negligible for this period. During the second period, a distinct increase of the loads could be noticed, up to 2.6 t/m for SMAG, 223 t/m for silt, and 785 t/m for CLAY on average. Generally, the CLAY fraction dominates the sediment loads introduced into the DR, reaching over 66% of the total load in June, when the maximum values during the year are observed.

Table 1. Average monthly sediment fraction loads for the Myślenice calculation profile for the baseline and variant scenarios (t/m).

	Baseline			VS1			VS2			VS3			VS4		
Month	SMAG	SILT	CLAY	SMAG	SILT	CLAY	SMAG	SILT	CLAY	SMAG	SILT	CLAY	SMAG	SILT	CLAY
Nov	0.00	2.0	108.6	0.00	1.2	80.3	0.00	1.7	111.5	0.00	1.1	92.2	0.00	1.4	112.3
Dec	0.00	0.2	52.5	0.00	4.0	162.3	0.00	2.3	168.1	0.00	2.4	147.0	0.00	3.9	170.8
Jan	0.00	0.4	65.2	0.00	1.2	99.8	0.00	0.4	108.0	0.00	1.2	107.0	0.00	0.6	108.3
Feb	0.00	5.3	165.9	0.00	28.9	245.9	0.00	22.1	442.0	0.00	29.3	235.4	0.00	27.6	557.8
Mar	0.00	23.9	430.5	0.00	9.2	484.9	0.00	19.8	755.1	0.00	15.2	471.4	0.06	53.0	762.9
Apr	0.00	5.3	545.3	0.04	99.7	1773.1	0.01	73.0	1621.0	0.05	117.1	1990.1	0.03	114.6	1957.1
May	0.93	122.3	1047.9	0.34	59.1	774.8	0.31	68.7	734.8	0.22	42.3	604.5	0.30	71.3	698.8
Jun	6.91	616.0	1224.0	6.88	512.6	1072.2	3.93	447.2	1023.4	3.76	376.1	887.5	3.09	301.4	850.0
Jul	1.95	213.3	745.4	0.82	157.7	599.8	0.53	105.4	518.7	0.58	136.0	502.7	0.48	127.6	553.3
Aug	3.44	130.2	571.3	0.37	61.4	326.5	0.11	26.6	217.9	1.17	78.2	367.9	1.73	103.2	427.9
Sep	0.10	34.1	337.6	0.01	13.5	216.0	0.02	15.4	234.2	0.01	7.5	193.6	0.07	34.3	264.6
Oct	0.00	7.3	170.8	0.01	24.9	311.5	0.04	49.3	395.6	0.02	24.1	286.8	0.02	23.1	255.3
average	1.11	96.7	455.4	0.71	81.1	512.2	0.41	69.3	527.5	0.48	69.2	490.5	0.48	71.8	559.9
CV	1.91	1.8	0.9	2.77	1.8	1.0	2.71	1.8	0.9	2.26	1.5	1.1	1.99	1.2	0.9

Under the variant scenarios (VS1-VS4) the temporal pattern of sediment loads has been generally maintained, with elevated values during the May-October period, and their decrease during the remaining months of the year (Table 1). However, differences in the scenarios' impact on particular sediment fractions should be noticed. For the SMAG fraction, a decrease of the loads under all discussed scenarios is visible when compared to the baseline scenario. For the remaining fractions, deviations from this pattern are apparent, especially for CLAY. An increase of the clay fraction loads is evident during the winter and spring months (except for May), reaching extreme values in April, elevated by 197-265% when compared to the baseline scenario. During the remaining months, an increase in September is also noticeable, by 49.5-131.6% of the baseline load. The similar

pattern of the load changes under the variant scenarios has been also detected for SILT, with the April loads for this fraction growing from 5.3 t/m, up to over 110 t/m under VS3 and VS4.

3.1.2. The Average High Discharges (AHQ)

The monthly AHQ values for the Myślenice calculation profile, subsequently used for the AdH/PTM module simulations, were obtained from the SWAT for the baseline and variant scenarios (Table 2). In the baseline scenario, the increase of the flow values can be observed from May to September, reaching up to 147 m3/s in June. During the remaining months of the year (October-April) the AHQ flows vary from 16 m3/s for December to 58 m3/s in October. Under the variant scenarios, the extension of the AHQ elevated values can be observed due to the increase of the flows from October to April, even by 45 m3/s for VS3 and VS4. During the remaining months the decrease of the AHQ can be observed, even by 49 m3/s in August for VS2).

Table 2. Monthly average AHQ values (m3/s) for the Myślenice calculation profile.

Month	Base	VS1	VS2	VS3	VS4
Nov	37	34	38	33	40
Dec	16	38	33	32	38
Jan	19	20	22	19	23
Feb	30	44	49	45	51
Mar	51	54	59	56	52
Apr	39	83	73	84	84
May	121	105	105	98	111
Jun	147	141	128	128	128
Jul	99	87	81	82	83
Aug	115	86	66	99	110
Sep	89	65	70	61	85
Oct	58	79	96	78	86

3.2. The Dobczyce Reservoir (DR) simulations

As a result of the AdH/PTM simulations, the percentages of each SMAG, SILT and CLAY fractions that were deposited in individual zones of the reservoir, under the baseline and variant scenarios, have been determined (Figure 6). Generally, on average over 86% of the all fractions flowing into the DR has been deposited within the reservoir in the baseline scenario, however, this process displayed a strong seasonal pattern, and also varied from fraction to fraction.

For SMAG, the presence of particles belonging to this fraction have been detected generally between May and September, with 26-47% of these particles deposited only in zone B of the DR, and 52-70% in C. The SMAG portion introduced into zone D was small, at the level of 0.2-3.8%, while the outflow of these particles from the DR (OUT) has been observed only in June, reaching 0.7% of the total SMAG particles. For the SILT fraction, the majority of these particles have been deposited into the first two zones of the DR (A and B), however, the share of particles in each zone displayed a seasonal pattern. From October to April, SILT particles were mostly retained in the first zone of the DR (A, 42-71%), while their share in the next zone was relatively smaller (B, 27-48%). In this period the share of this fraction reaching zone C was at the level of 2-9%, while their further transport into zones D and OUT was almost negligible. In the remaining months of the year, May-September, the SILT particles have been mainly deposited into zone B (67-72%), and partially into C (16-23%). The transport and deposition of this fraction into zones D and OUT was at the level of 1-4%. For the CLAY, a similar seasonal pattern could be observed, however, the localization of these particles' final deposition zones differs from the SILT fraction. Generally, between October and April these particles are deposited into zones B and C (23-47% and 30-40%, respectively), while the share reaching D is estimated at 4-13%. Also, the elevated share of CLAY particles transported downstream from the reservoir (OUT) should be noticed in October, November, and March (17-35%). For the May-September period, this process of particle transport downstream from the reservoir dominates, with 46-60% of the total number of CLAY particles estimated in the OUT zone. The remaining share of these particles is distributed between zones B, C, and D, with higher values for C (19-23%).

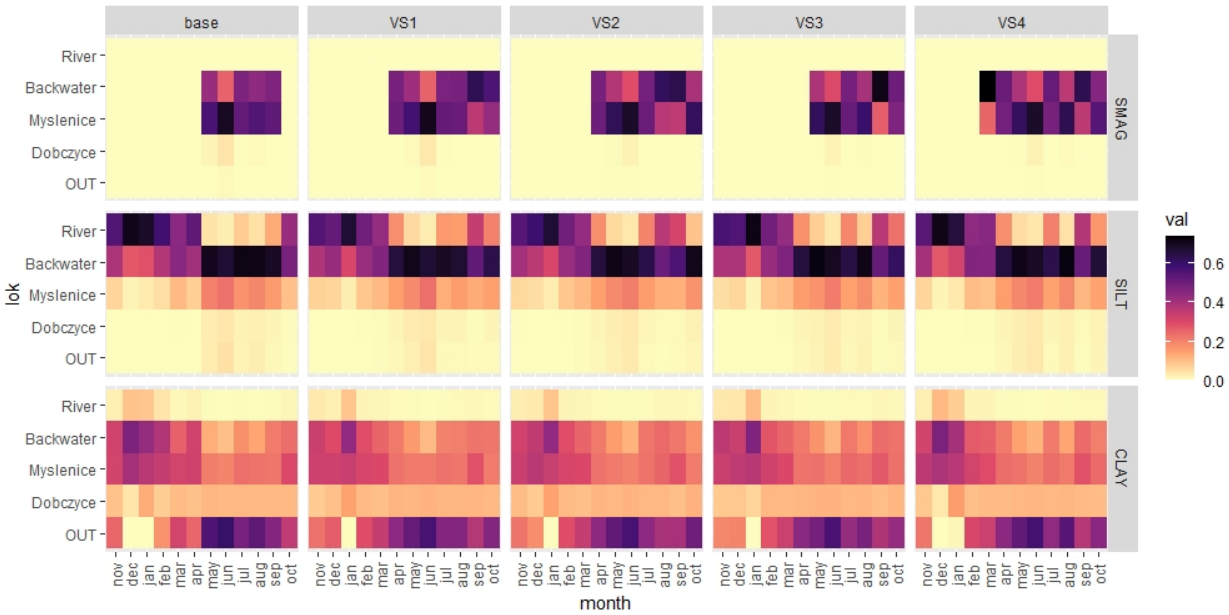

Figure 6. Percentage shares of the sediment fractions (SMAG, SILT, CLAY) deposited in the individual Dobczyce Reservoir zones.

The impact of the adopted variant scenarios on the SMAG section is expressed by the extension of the period when these particles are transported and deposited into the DR. For the baseline scenario these processes were confined to May-September, while under the VS1-VS3 scenarios also April and October are marked with SMAG deposition into the DR zones B and C. While under VS4, March is also included in this process. As for other zones of the DR, the share of these particles was either 0 (A), or at the level similar to the baseline scenario (0.1-3.3%). For the SILT fraction, the similar pattern of temporal changes could be expected under VS1-VS4. Although the majority of these particles will still be deposited into the first two DR zones, the period when particles are retained in zone A will be shortened from October-April to November-March to favor a higher percentage of particles settling into zone B (on average by 21%). For the CLAY fraction, the variant scenario impact is expressed mainly by extension of the period in which these particles flow downstream of the DR (OUT). In the baseline scenario, this process lasted from March to November, while in the VS1-VS3 scenarios December and January are also marked as meaningful for the CLAY particle transport to the lower part of the Raba River. In turn, from May to September the amount of the CLAY fraction reaching OUT will decrease by an average of 9%, depositing these particles mainly into zones B, C, and D.

Discussion

Dammed reservoirs pose a huge impact on entire aquatic ecosystems disrupting many natural processes, including sediment transport within the river through its effective entrapment [e.g. Sundborg, 1992; Vörösmarty et al., 2003; Sedláček et al., 2017; Dong et al., 2019]. Excessive sediment deposition threatens, not only reservoir capacity and functionality, but also creates an additional threat to the reservoir water quality since sediment particles are considered effective carriers of contaminants [e.g., Szalińska et al., 2013; Zhu et al., 2019; Jalowska and Yuan, 2019; Aradpour et al., 2020; Babek et al., 2020]. For a holistic assessment of sediment inflow impact on a reservoir, exhaustive information on its catchment as a sediment source is required. In the current study such information has been collected through previous research performed on the Raba River catchment for the land and river phases of the sediment transport [Orlińska-Woźniak et al., 2020; Szalińska et al., 2020]. Briefly, the mountainous part of this catchment located upstream from the Dobczyce Reservoir is very prone to erosion, therefore, multiple anti-erosion structures were constructed in 70's along the main river and its tributaries. However, currently the majority of these structures are overfilled and require renovation [Korpak et al., 2008; Lenar-Matyas et al., 2015]. The mountainous character of this area also demonstrates the hydrometeorological conditions typical for the entire area of the Polish Carpathian Mts., with average rainfall values reaching 1600 mm accompanied by frequent torrential rains, especially during the summer. These conditions combined with a high share of slopes above 25%, and many areas still used for agriculture (41%), cause intensive loss of soil fractions from the land phase of the catchment. Moreover, they are the reasons behind large fluctuations in flows and frequent floods affecting sediment transport in the river bed [Kijowska-Strugała and Kiszka, 2018]. These features had a decisive impact on sediment loads introduced into the DR simulated for the Myślenice calculation profile with the first module of the DNS digital platform - SWAT.

The obtained results showed high sediment loads, average of 184 t/m, displaying elevated temporal variability, with an average coefficient of variation (CV) of 153%. During the year, two periods can be distinguished: May-September when over 76% of the total annual sediment load flows through the Myślenice profile, and October-April when the rest of this load is delivered to the DR. As for the share of the individual fractions, mineral fine particles constitute over 99% of the total load, with CLAY and SILT contributing 82% and 17%, respectively. Such a dominant share of these fractions results from the natural conditions in the studied catchment [Szarek-Gwiazda

and Sadowska, 2010], where clay soils cover more than 95% of the area (Figure 2). Moreover, frost lasting more than 100 days per year in this part of the Carpathian Mts. also promotes erosion of soils, especially of those fine-grained. The high content of fine fractions facilitates groundwater capillary forces, causing exfoliation of the surface layers during periods of freezing temperatures [Augustowski and Kukulak, 2017]. Apart from the two mineral fractions (CLAY and SILT), a small amount of mineral-organic agglomerates (SMAG) also has been observed (0.2%), mostly during the May-August period. The period of their appearance coincides with the period of high flows, but also favorable conditions for the biomass production in the river (e.g., temperature, solar radiation, and agricultural activities) [Lee et al., 2019; Hoffman et al., 2020].

The subsequent fate of the sediment particles downstream from the Myślenice calculation profile has been tracked with the second module of the DNS digital platform, AdH/PTM. Due to the RR width increase in the outlet section and the water flow decrease, zone A favors deposition of larger particles. Although the SWAT model practically did not simulate mineral fractions above 0.062 mm in our approach, due to the natural catchment conditions and the choice of the Kodoatie sediment transport routing method, as more suitable for suspended sediment simulations [Yen et al., 2017], extensive sandbanks are noticeable in the mouth of the RR (Figure 3). This phenomenon is caused by a combination of multiple natural features and processes, including presence of less fine-grained soils in the last sub-catchment of the RR (Figure 2), and urban use in this part of the area, supplying sand particles due to construction work and winter maintenance of the local roads. Moreover, other mineral particles lose their driving force of advection and begin to settle in this zone, especially during the October-April period, when the average flow (av. 35 m^3/s) favors the deposition of 60% of all sediment particles (56% of SILT and 4% of CLAY) (Figure 7). With the increasing flow, up to 114 m^3/s on average during the May-September period, sediment deposition is limited to only 6% of their total load.

In zone B, the DR water level fluctuations result in alternating cycles of sedimentation and resuspension in this part of the DR (backwater) [Szlapa and Hachaj, 2017]. As a consequence, deposition of particles not settled in zone A is favored here. Especially of the SILT larger fractions (Figure 7), which are retained up to 70% during the May-September period. For the finer particles of the CLAY fraction, this zone is also the major deposition zone (34%), especially during the lower flow period (October-April). Furthermore, over 40% of the SMAG fraction is deposited during the May to September period in this zone. Due to their lower density, SMAG particles are larger than mineral particles of the same mass which results in their slower

settling velocity and higher drag force [Hoffmann et al., 2020]. As a consequence, SMAG particles can be transported much further than mineral particles of the same mass, which explains the lack of their deposition in zone A.

In zone C, with depth increasing to over 9 m and flow continuing to decline, the sediment-carrying potential becomes even weaker. This zone is the last which receives large amounts of SILT fractions (up to 18% on average in May-September), and accumulates over 57% of the SMAG particles. Moreover, a distinctive pattern of bedforms, created by the settling particles, is noticeable in this zone in the form of numerous ripple marks (Figure 7). Behind each of them, planar velocity drops and a local downward velocity component appears. This causes the particle accumulation in the form of underwater dunes with bigger grains deposited on the stoss side (represented by more orange shades), and smaller ones on the lee side (colored more towards red). Furthermore, each of the subsequent dunes accumulates (on average) finer material than the previous one. A similar pattern of bedforms is also visible for the SMAG particles (Figure 7)

The last zone of the DR (D), is characterized by the greatest depth (over 16 m) and the presence of the drinking water intake. During high flows (May-September) even more than 60% of the CLAY fraction load flows into this zone, which requires special attention due to the adsorption of contaminants on fine particles [Szalińska et al., 2013; Palma et al., 2015; Rügner et al., 2019]. Since only 10% of this load settles into this part of the DR, it is not really prone to the loss of capacity. However, the remaining particles are transported downstream of the DR (OUT) to the lower part of the RR catchment.

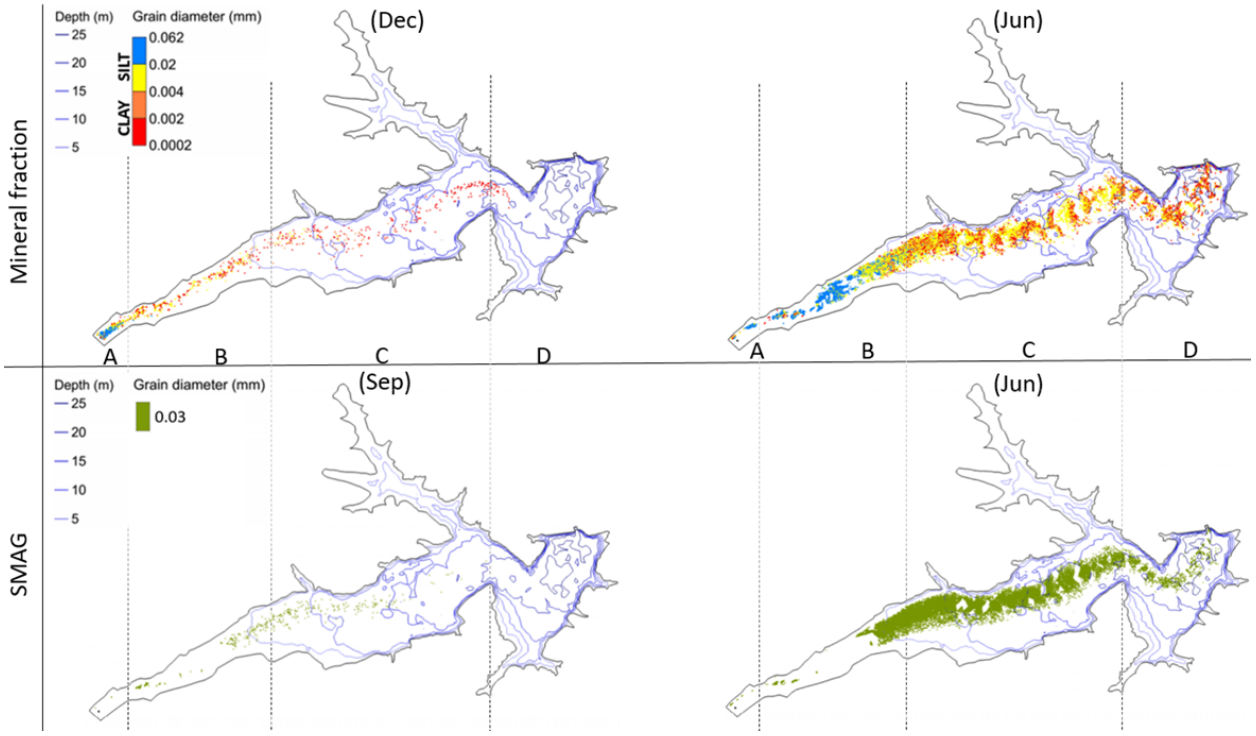

Figure 7. Sediment fraction distribution in the Dobczyce Reservoir under the baseline scenario.

The impact of the future climate changes, for the land and river phases of the sediment transport in the RR catchment, has underlined the role of the spring and winter season, mainly due to the increase of precipitation [Orlińska-Woźniak et al., 2020; Szalińska et al., 2020]. Moreover, the detailed simulations [Hachaj et al., 2021] have shown that such increases of sediment yields and loads could not be attenuated by the forecasted land use changes in this area, e.g., 30% increase of forest area at the expense of agricultural land use. In the current study, where the climate change predictions with a monthly step were applied, a more detailed temporal pattern of sediment transport has been elucidated. In particular, a considerable increase of precipitation observed especially in April (up to 81% under VS4), but also in December, February, and October (up to 76% under VS1) in all the discussed scenarios (Figure 5), will ultimately affect the mineral and organic fraction of sediments delivered into the Myślenice calculation profile. Currently (baseline scenario), during these four months, a total of just over 18 t/m of SILT, and 934 t/m of CLAY flows through this profile. Whereas the future climate changes will lead in these months to the average

SILT load increase by 154 t/m (VS3), and by more than 2000 t/m (VS4) for CLAY. Since the pattern of precipitation changes will be reversed during May-September (Figure 5), a decrease of sediment loads in the Myślenice profile can be expected in these months, when compared to the baseline scenario. Indeed, the load of transported fractions will be reduced in these months by 430 and 1160 t/m for SILT and CLAY, respectively. These monthly changes require further attention, however, it has been already recognized that this area is likely to experience substantial climate exposure leading to further alterations in the ecosystem [Hlasny et al., 2016].

The climate change scenarios applied to the reservoir simulations emphasize a fundamental difference between both parts of the discussed system. While even a small change of parameters (such as precipitation, temperature, or land cover) causes a rapid hydrological reaction of the mountainous river catchment; and consequently alters the intensity of erosion, and sediment transport, and fate; the response of the reservoir is very disparate. The flow velocity field, which is crucial for the range of the sediment particles transport, remains sensitive to flow rate changes only in zones A and B of the DR (river and backwater). Therefore, these two zones will remain the main depositional sections of the DR, especially for larger particles, even under flood conditions [Szlapa 2019]. Directly behind the backwater zone, the sudden extension of the reservoir's cross-sectional area and a slowdown of the water flow, radically changes the sediment transport possibilities in further parts of the DR. Therefore, when the SILT fraction behavior in the DR is discussed, only changes in particle numbers and a slight shift in temporal pattern in zones A and B can be noticed. Regardless of the selected scenario, a pronounced increase, by an astounding 800%, of the SILT fraction can be expected in these two zones (Table 1, Figure 8). As for the monthly distribution, since the high-flow period has been extended from May-September in the baseline scenario, to April-October in the V1-V4 scenarios, therefore, a similar extension in retention effectiveness of SILT particles in zone B is visible (Figure 8). This leads towards increasing the rate of the reservoir volume loss in time, and consequently causes a transition of the backwater zone (B) towards the dam at the cost of the intermediate zone (C). The lacustrine zone (D) stays unaffected by this SILT rate increase. Moreover, a similar pattern is also noticeable for the SMAG particles. Although their spatial pattern remains the same under the adapted scenarios, i.e., their appearance is restricted only to zones B and C, their temporal distribution is noticeably different, as it is extended to include even March under V4. It should be also noted that an extended period of allochthonous organic material delivery to the reservoir can promote further development of the autochthonous organic matter due

to the favorable conditions in the DR [Szlapa et al., 2017]. As for the CLAY particles, the reservoir response to the applied scenarios will completely differ. The altered high flow period, April-October, will increase the mobility of these particles, pushing them to flow to the last reservoir zone (D), and even downstream from the reservoir (OUT). Generally, the share of this fraction flowing to zone D will be increased even by 30% (December) when compared to the baseline scenario, but only an average of 10% of them will settle there. Since this zone is used as a source of drinking water, the extended presence in this part of the reservoir should be further investigated due to their role as a contaminant carrier, as previously discussed [Szalińska et al., 2021].

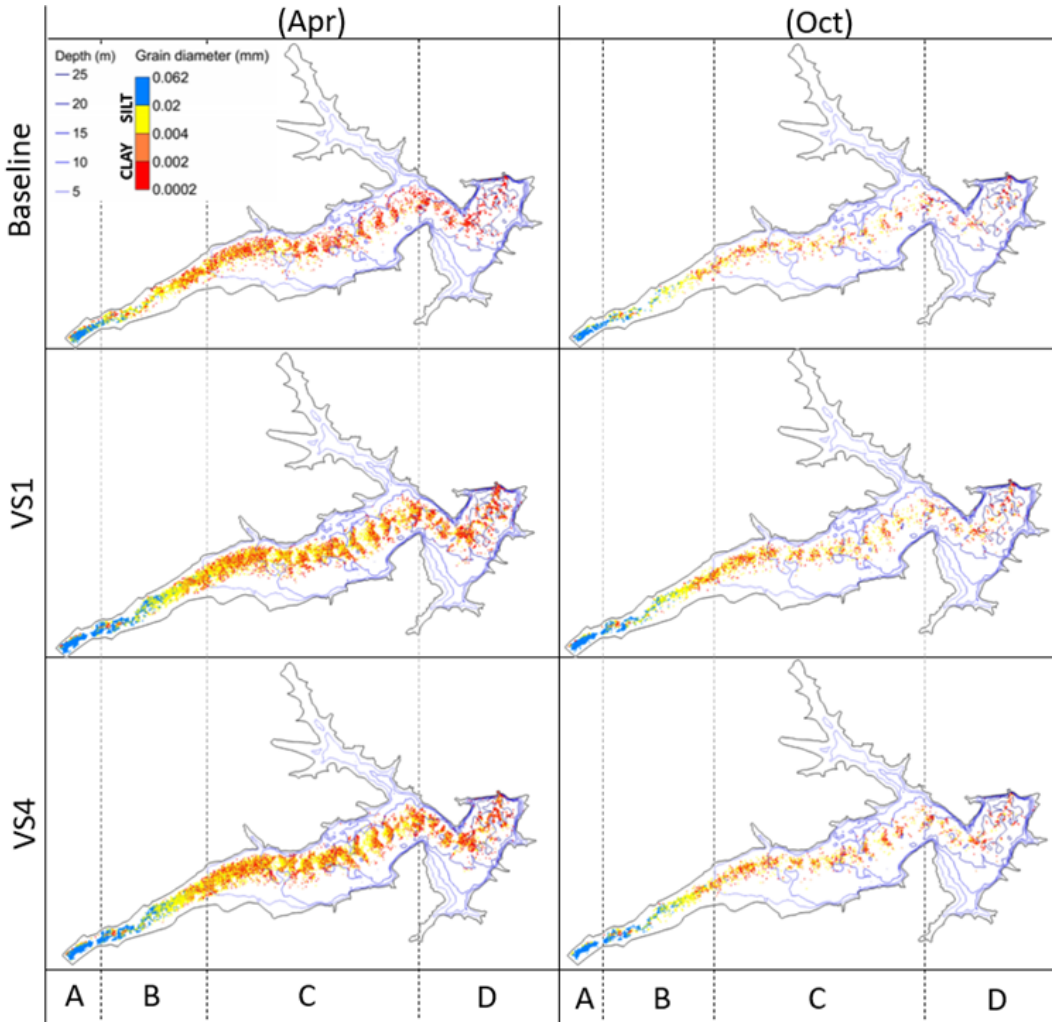

Figure 8. Sediment fractions' distribution in the Dobczyce Reservoir under the selected variant scenarios (VS1 and VS4).

Conclusions

In the current study we have tracked the selected fractions of sediment particles (SMAG, SILT, and CLAY) from their source of origin (Raba River catchment) to the deposition area being in a dammed reservoir (Dobczyce Reservoir). This research was possible due to the combined performance of two models (SWAT and AdH/PTM) under the umbrella of the Macromodel DNS digital platform. The results underlined the fundamental difference between both hydrological units, i.e., river catchment and dammed reservoir. Although the studied river catchment is extremely prone to erosion, and under the forecasted climate change will respond in increasing sediment loads, this response will eventually be attenuated by the reservoir. Due to the very fortunate location and natural setup of the studied reservoir, the two first zones will maintain their trapping role for the larger particles (SILT), even during periods of highly increased sediment delivery periods under the adopted climate and land use scenarios. Although, special attention must be paid towards acceleration of the capacity loss for this part of the reservoir. As for the finer particles (CLAY), their increased mobility into the reservoir is clearly visible both under short- and long-term scenarios which raises concerns due to their contaminant binding affinity, and possible impact on drinking water. Moreover, our study clearly shows that a seasonal approach to climate change predictions is quite distorted, and monthly predictions are recommended, especially when necessary measures to evaluate sediment fate in a catchment are discussed.

Acknowledgements

This research was supported by: AGH (sub. 16.16.140.315), CUT (2020 sub. for Dept. of Geoengineering Water Management), and IMGW-PIB (sub. FBW-6 and 7). The study was performed out as part of the Interdisciplinary Research Group - Pollutant Transport in a Catchment (http://ochrsrod.agh.edu.pl/index.html) activity. For the Raba catchment modeling part, the ArcGIS software (version 10.2.1) by ESRI (https://www.esri.pl/arcgis/) and The Soil & Water Assessment Tool (SWAT - version 2012 - https://swat.tamu.edu/software/swat-executables/) were used. The input data for this model and its calibration parameters for the Raba catchment are described in detail in [Szalińska et al., 2020 - https://doi.org/10.1007/s11368-020-02600-8; Orlińska-Woźniak et al., 2020a - https://doi.org/10.3390/w12051499]. The SWAT-CUP program was used to calibrate the SWAT model - version 2019, 5.2.1.1 for Windows (https://www.2w2e.com/home/SwatCup) and LOADEST from the U.S. Geo-

logical Survey (USGS) (https://water.usgs.gov/software/loadest/). The final output from the SWAT sediment model for the Raba River catchment area was published in the Mendeley database - https://data.mendeley.com/datasets/rft94c75zb/3. For the Dobczyce Reservoir modeling part, the AdH and PTM models (parts of SMS framework version 13.0) by AQUAVEO (https://www.aquaveo.com/) were used. The input data for the models and implementation on the object are described in detail in [Szlapa 2019 - http://suw.biblos.pk.edu.pl/resourceDetailsBPP&rId=91036; Hachaj 2018 - https://doi.org/10.15244/pjoes/78675 ; Szlapa and Hachaj, 2017 - https://doi.org/10.4467/2353737XCT.17.112.6653]. The validation of the models was presented in [Hachaj 2019] - AdH model and [Szlapa 2019] - PTM module. The output from the PTM model for the Dobczyce Reservoir was published in the Mendeley database - https://data.mendeley.com/datasets/k9c7c666bt/1

References

Aksoy, H., Mahe, G., Meddi, M. (2019). Modeling and practice of erosion and sediment transport under change. Water, 11(8), 1665. https://doi.org/10.3390/w11081665

Antoine, G., Camenen, B., Jodeau, M., Némery, J., Esteves, M. (2020). Downstream erosion and deposition dynamics of fine suspended sediments due to dam flushing. Journal of Hydrology, 585, 124763. https://doi.org/10.1016/j.jhydrol.2020.124763

Aradpour, S., Noori, R., Tang, Q., Bhattarai, R., Hooshyaripor, F., Hosseinzadeh, M., Torabi Haghighi, A., Klöve, B. (2020). Metal contamination assessment in water column and surface sediments of a warm monomictic man-made lake: Sabalan Dam Reservoir, Iran. Hydrology Research, 51(4), 799-814. https://doi.org/10.2166/nh.2020.160

Arnold, J. G., Moriasi, D. N., Gassman, P. W., Abbaspour, K. C., White, M. J. (2012). SWAT: Model use, calibration, and validation. Transactions of the ASABE, 55(4), 1491-1508. 10.13031/2013.42256

Abbaspour, K.C., Rouholahnejad, E., Vaghefi, S.R., Srinivasan, R., Yang, H., Kløve, B. (2015) A continental-scale hydrology and water quality model for Europe: Calibration and uncertainty of a high-resolution large-scale SWAT model. J. Hydrol. 524, 733–752. https://doi.org/10.1016/j.jhydrol.2015.03.027

Augustowski, K., Kukulak, J. (2017). Rates of frost erosion in river banks with different particle size (West Carpathians, Poland). Geografia Fisica e Dinamica Quaternaria, 40, 5-17. 10.4461/GFDQ.2017.40.1

Ayaseh A, Salmasi F, Dalir AH, Arvanaghi H (2019) A performance comparison of CCHE2D model with empirical methods to study sed-

iment and erosion in gravel-bed rivers. Int J Sci Environ Technol 16(12):7933–7942. https://doi.org/10.1007/s13762-019-02229-2

Banasik, K., Skibinski, J., Gorski, D. (1993). Investigation on sediment deposition in a designed Carpathian reservoir. IAHS publication, 101-101.

Bábek, O., Kielar, O., Lenďáková, Z., Mandlíková, K., Sedláček, J., Tolaszová, J. (2020). Reservoir deltas and their role in pollutant distribution in valley-type dam reservoirs: Les Království Dam, Elbe River, Czech Republic. Catena, 184, 104251. https://doi.org/10.1016/j.catena.2019.104251

Berger R.C, Tate J.N, Brown G.L Savant G, Adaptive hydraulics users manual. AQUA- VEO, 2010.

Berteni, F., Grossi, G. (2020). Water Soil Erosion Evaluation in a Small Alpine Catchment Located in Northern Italy: Potential Effects of Climate Change. Geosciences, 10(10), 386. https://doi.org/10.3390/geosciences10100386

Bladé Castellet, E., Sánchez-Juny, M., Arbat Bofill, M., Dolz Ripollès, J. (2019). Computational modeling of fine sediment relocation within a dam reservoir by means of artificial flood generation in a reservoir cascade. Water Resources Research, 55(4), 3156-3170. https://doi.org/10.1029/2018WR024434

Bilali, A. E., Taleb, A., Idrissi, B. E., Brouziyne, Y., Mazigh, N. (2020). Comparison of a data-based model and a soil erosion model coupled with multiple linear regression for the prediction of reservoir sedimentation in a semi-arid environment. Euro-Mediterranean Journal for Environmental Integration, 5(3), 1-13. https://doi.org/10.1007/s41207-020-00205-8

Borrelli, P., Van Oost, K., Meusburger, K., Alewell, C., Lugato, E., & Panagos, P. (2018). A step towards a holistic assessment of soil degradation in Europe: Coupling on-site erosion with sediment transfer and carbon fluxes. Environmental Research, 161, 291-298. https://doi.org/10.1016/j.envres.2017.11.009

Borrelli, P., Robinson, D. A., Panagos, P., Lugato, E., Yang, J. E., Alewell, C., Wuepper, D., Montanarella, L., Ballabio, C. (2020). Land use and climate change impacts on global soil erosion by water (2015-2070). Proceedings of the National Academy of Sciences, 117(36), 21994-22001. https://doi.org/10.1073/pnas.2001403117

Burgan, H. I., Icaga, Y. (2019). Flood analysis using Adaptive Hydraulics (AdH) model in Akarcay Basin. Teknik Dergi, 30(2), 9029-9051. https://doi.org/10.18400/tekderg.416067

Ciampalini, R., Constantine, J. A., Walker-Springett, K. J., Hales, T. C., Ormerod, S. J., Hall, I. R. (2020). Modelling soil erosion responses to climate change in three catchments of Great Britain. Science of the Total Environment, 749, 141657. https://doi.org/10.1016/j.scitotenv.2020.141657

Charafi, M. M. (2019). Two-dimensional numerical modeling of sediment transport in a dam reservoir to analyze the feasibility of a water intake. International Journal of Modern Physics C, 30(01), 1950003. https://doi.org/10.1142/S0129183119500037

Croley, T. E., Raja Roa, K. N., Karim, F. (1978). Reservoir sedimentation model with continuing distribution, compaction and slump (IIHR Report no. 198). Iowa City, IA: Iowa Institute of Hydraulic Research, The University of Iowa.

Czuba, J. A., Straub, T. D., Curran, C. A., Landers, M. N., Domanski, M. M. (2015). Comparison of fluvial suspended-sediment concentrations and particle-size distributions measured with in-stream laser diffraction and in physical samples. Water Resources Research, 51(1), 320-340. https://doi.org/10.1002/2014WR015697

Dibike, Y., Shakibaeinia, A., Eum, H. I., Prowse, T., Droppo, I. (2018). Effects of projected climate on the hydrodynamic and sediment transport regime of the lower Athabasca River in Alberta, Canada. River Research and Applications, 34(5), 417-429. https://doi.org/10.1002/rra.3273

Dong, J., Xia, X., Liu, Z., Zhang, X., Chen, Q. (2019). Variations in concentrations and bioavailability of heavy metals in rivers during sediment suspension-deposition event induced by dams: insights from sediment regulation of the Xiaolangdi Reservoir in the Yellow River. Journal of Soils and Sediments, 19(1), 403-414. https://doi.org/10.1007/s11368-018-2016-1

Dosio, A., 2016. Projections of climate change indices of temperature and precipitation from an ensemble of bias-adjusted high-resolution EURO-CORDEX regional climate models. J. Geophys. Res.-Atmos. 121 (10), 5488–5511. https://doi.org/10.1002/2015JD024411.

Feng, M., Shen, Z. (2021). Assessment of the Impacts of Land Use Change on Non-Point Source Loading under Future Climate Scenarios Using the SWAT Model. Water, 13(6), 874. https://doi.org/10.3390/w13060874

Garg, V., Jothiprakash, V. (2010). Modeling the time variation of reservoir trap efficiency. Journal of Hydrologic Engineering, 15(12), 1001–1015. https://doi.org/10.1061/(ASCE)HE.1943-5584.0000273

Gianinetto, M., Aiello, M., Vezzoli, R., Polinelli, F. N., Rulli, M. C.,

Chiarelli, D. D., Bocchiola, D., Ravazzani, G., Soncini, A. (2020). Future scenarios of soil erosion in the Alps under climate change and land cover transformations simulated with automatic machine learning. Climate, 8(2), 28. https://doi.org/10.3390/cli8020028

Gorczyca, E., Krzemień, K., Sobucki, M., Jarzyna, K. (2018). Can beaver impact promote river renaturalization? The example of the Raba River, southern Poland. Science of the Total Environment, 615, 1048-1060. https://doi.org/10.1016/j.scitotenv.2017.09.245

Green, W. R., Robertson, D. M. and Wilde, F. D. (2015) 'USGS National Field Manual for the Collection of Water-Quality Data; Lakes and Reservoirs: Guidelines for Study Design and Sampling', in Techniques of Water-Resources Investigations Book 9. Reston, Virginia, p. 65. doi:

0.3133/tm9a10

Guillén Ludeña, S., Cheng, Z., Constantinescu, G., Franca, M.J. (2017). Hydrodynamics of mountain-river confluences and its relationship to sediment transport. Journal of Geophysical Research: Earth Surface, 122(4), 901-924. https://doi.org/10.1002/2016JF004122

Hachaj, P.S., Szlapa, M. (2017). Impact of a thermocline on water dynamics in reservoirs–Dobczyce reservoir case. Archive of Mechanical Engineering, 64(2), 189-203. 10.1515/meceng-2017-0012

Hachaj, P.S. (2018). Preliminary results of applying 2D hydrodynamic models of water reservoirs to identify their ecological potential. Polish Journal of Environmental Studies, 27(5), 2049–2057. https://doi.org/10.15244/pjoes/78675

Hachaj, P.S. (2019). Analysis of dammed reservoir hydrodynamics for water management purposes : the model and its use cases, Cracow University of Technology. (in Polish)

Hachaj, P. S., Kołodziejczyk, K. (2020). Usefulness of sentinel-2 visible light satellite photos for surveys of hydrodynamic phenomena in polish carpathian storage reservoirs. *Carpathian Journal of Earth and Environmental Sciences*, *15*(1), 197–210. https://doi.org/10.26471/cjees/2020/015/122

Hachaj, P. S., Szlapa, M., Orlińska-Woźniak, P., Jakusik, E., Wilk, P., Szalińska, E. (2021), "Sediment particle distribution in a dammed reservoir under climate and land use scenarios (Carpathian Mts.)", Mendeley Data, http://dx.doi.org/10.17632/k9c7c666bt.1

Halecki,W., Kruk, E., Ryczek, M. (2018a) Loss of topsoil and soil erosion by water in agricultural areas: A multi-criteria approach for various land use scenarios in theWestern Carpathi-

ans using a SWAT model. Land Use Policy, 73, 363–372. https://doi.org/10.1016/j.landusepol.2018.01.041

Halecki, W., Kruk, E., & Ryczek, M. (2018b). Evaluation of water erosion at a mountain catchment in Poland using the G2 model. Catena, 164, 116-124. https://doi.org/10.1016/j.catena.2018.01.014

Hlasny, T., Trombik, J., Dobor, L., Barcza, Z., Barka I. (2016). Future climate of the Carpathians: climate change hot-spots and implications for ecosystems. Reg Environ Change, 16, 1495–1506.

https://doi.org/10.1007/s10113-015-0890-2

Hoffmann, T.O., Baulig, Y., Fischer, H., Blöthe, J. (2020). Scale-breaks of suspended sediment rating in large rivers in Germany induced by organic matter. Earth Surf. Dynam., 8, 661–678. https://doi.org/10.5194/esurf-8-661-2020

Hohmann, C., Kirchengast, G., Birk, S. (2018). Alpine foreland running drier? Sensitivity of a drought vulnerable catchment to changes in climate, land use, and water management. Climatic change, 147(1), 179-193. https://doi.org/10.1007/s10584-017-2121-y

Hu, D., Li, S., Jin, Z., Lu, S., Zhong, D. (2021). Sediment transport and riverbed evolution of sinking streams in a dammed karst river. Journal of Hydrology, 596, 125714. https://doi.org/10.1016/j.jhydrol.2020.125714

Huang, C. C., Chang, M. J., Lin, G. F., Wu, M. C., Wang, P. H. (2021). Real-time forecasting of suspended sediment concentrations reservoirs by the optimal integration of multiple machine learning techniques. Journal of Hydrology: Regional Studies, 34, 100804. https://doi.org/10.1016/j.ejrh.2021.100804

Idrees, M. B., Jehanzaib, M., Kim, D., Kim, T. W. (2021). Comprehensive evaluation of machine learning models for suspended sediment load inflow prediction in a reservoir. Stochastic Environmental Research and Risk Assessment, 1-19. https://doi.org/10.1007/s00477-021-01982-6

Jalowska, A. M., Yuan, Y. (2019). Evaluation of SWAT impoundment modeling methods in water and sediment simulations. JAWRA Journal of the American Water Resources Association, 55(1), 209-227. https://doi.org/10.1111/1752-1688.12715

Jiang, J., Liang, Q., Xia, X., Hou, J. (2021). A coupled hydrodynamic and particle-tracking model for full-process simulation of nonpoint source pollutants. Environmental Modelling & Software, 136, 104951. https://doi.org/10.1016/j.envsoft.2020.104951

Kijowska-Strugała, M., Wiejaczka, Ł., Gil, E., Bochenek, W.,

Kiszka, K. (2017) The impact of extreme hydro-meteorological events on the transformation of mountain river channels (Polish Flysch Carpathians). Ann. Geomorphol., 61, 75–89. https://doi.org/10.1127/zfg/2017/0434

Kijowska-Strugała, M., Kiszka, K. (2018). Environmental factors affecting splash erosion in the mountain area (the Western Polish Carpathians). Landform Analysis, 36. doi: 10.12657/landfana.036.009

Kimmel, B. L., Lind, O. T., Paulson, L. J. (1990). Reservoir primary production. In K. W. Thornton, B. L. Kimmel, F. E. Payne (Eds.), Reservoir Limnology (pp. 133–194). John Wiley & Sons, Inc.

Kędra, M., Szczepanek, R. (2019). Land cover transitions and changing climate conditions in the Polish Carpathians: Assessment and management implications. Land Degradation & Development, 30(9), 1040-1051. https://doi.org/10.1002/ldr.3291

Kodoatie RJ (2000) Sediment transport relations in alluvial channels. Unpublished PhD Thesis. Colorado State University, Colorado, USA

Korpak, J., Krzemien, K., Radecki-Pawlik, A. (2008). Influence of anthropogenic factors on changes of Carpathian stream channels. Infrastruct. Ecol. Rural Areas 2008, 4, 249–260.

Kozak, J., Urs, G., Thomas, H., Janine, B., 2017. Current practices and challenges for modelling

past and future land use and land cover changes in mountainous regions. Reg. Environ. Chang. 17, 2187–2191. https://doi.org/10.1007/s10113-017-1217-2.

Lee, B. J., Kim J., Hur J., Choi, I. H., Toorman, E., Fettweis, M., Choi, J.W. (2019). Seasonal Dynamics of Organic Matter Composition and Its Effects on Suspended Sediment Flocculation in River Water. Water Resources Research, 55(8), 6968-6985. https://doi.org/10.1029/2018WR024486

Lenar-Matyas, A., Korpak, J., Mączałowski, A., Wolanski, K. (2015). Changes in the Krzczonówka stream cross-sections after passing flood discharge. Infrastruct. Ecol. Rural Areas, 4, 965–977.

Lu, S., Kronvang, B., Audet, J., Trolle, D., Andersen, H. E., Thodsen, H., van Griensven, A. (2015). Modelling sediment and total phosphorus export from a lowland catchment: Comparing sediment routing methods. Hydrological processes, 29(2), 280-294. https://doi.org/10.1002/hyp.10149

Luong, T. T., Pöschmann, J., Kronenberg, R., Bernhofer, C. (2021).

Rainfall Threshold for Flash Flood Warning Based on Model Output of Soil Moisture: Case Study Wernersbach, Germany. doi: 10.20944/preprints202103.0185.v1

Mazurkiewicz-Boron, G. (2016) Catchment conditions, chemistry, and water trophies. In The Dobczyce Reservoir; Sadag, T., Bandula, T., Materek, E., Mazurkiewicz-Boron, G., Slonki, R., Eds. Attyka: Krakow, Poland, 147–153. (In Polish)

MacDonald, N. J., Davies, M. H., Zundel, A. K., Howlett, J. D., Demirbilek, Z., Gailani, J. Z., Lackey, Tahirih C., Smith, J. (2006). PTM: particle tracking model. Report 1: Model theory, implementation, and example applications. Engineer Research And Development Center Vicksburg Ms Coastal And Hydraulics Lab.

Mikuś, P., Wyżga, B., Walusiak, E., Radecki-Pawlik, A., Liro, M., Hajdukiewicz, H., Zawiejska, J. (2019). Island development in a mountain river subjected to passive restoration: The Raba River, Polish Carpathians. Science of the Total Environment, 660, 406-420. https://doi.org/10.1016/j.scitotenv.2018.12.475

Mostowik, K., Siwek, J., Kisiel, M., Kowalik, K., Krzysik, M., Plenzler, J., Rzonca, B. (2019). Runoff trends in a changing climate in the Eastern Carpathians (Bieszczady Mountains, Poland). Catena, 182, 104174. https://doi.org/10.1016/j.catena.2019.104174

MPA (2021a). Development of urban adaptation plans for cities with more than 100,000 inhabitants in Poland. http://44mpa.pl/project-background/?lang=en (accessed 20.02.2021).

MPA (2021b). MPA project – urban adaptation plans. http://klimada.mos.gov.pl/en/ (accessed 20.02.2021).

Neil J. MacDonald, Demirbilek, Z., Joseph, Z., Gailani, C., Lackey, S, Smith, J., (2006) PTM: Particle Tracking Model, Coastal and Hydraulics Laboratory, U.S. Army Corps of Engineers, Vicksburg.

Neitsch, S. L., Arnold, J. G., Kiniry, J. R., Williams, J. R. (2011). Soil and water assessment tool theoretical documentation version 2009. Texas Water Resources Institute.

Operacz, A. (2017). The term "effective hydropower potential" based on sustainable development–an initial case study of the Raba river in Poland. Renew. Sustain. Energy, 75, 1453–1463. http://dx.doi.org/10.1016/j.rser.2016.11.141

Orlińska-Woźniak, P., Szalińska, E., Wilk, P. (2020a). Do Land Use Changes Balance out Sediment Yields under Climate Change Predictions on the Sub-Basin Scale? The Carpathian Basin as an Example. Water, 12(5), 1499. https://doi.org/10.3390/w12051499

Orlińska-Woźniak, P., Szalińska, E., Wilk, P. (2020b). A macromodel dns/swat dataset for the sediment yield analysis in the raba river basin (Carpathian mts.). Data in Brief, 33, 106574. https://doi.org/10.1016/j.dib.2020.106574

Palma, P., Ledo, L., Alvarenga, P. (2015). Assessment of trace element pollution and its environmental risk to freshwater sediments influenced by anthropogenic contributions: the case study of Alqueva reservoir (Guadiana Basin). Catena, 128, 174-184. https://doi.org/10.1016/j.catena.2015.02.002

Partyka, A. The preliminary estimation of the load of floated rubble transported by the Raba across the water-level indicator cross-section of the river in Stró˙za in the period 22–28 July 2001. Gospod. Wodna 2002, 10, 422–425.

Price, B., Kaim, D., Szwagrzyk, M., Ostapowicz, K., Kolecka, N., Schmatz, D.R., Wypych, A., Kozak, J., (2017). Legacies, socio-economic and biophysical processes and drivers: the case of future forest cover expansion in the Polish Carpathians and Swiss Alps. Reg. Environ. Chang. 17 (8), 2279–2291. https://doi.org/10.1007/s10113-016-1079-z.

Rummukainen, M., 2016. Added value in regional climate modeling.WIRES Clim. Change 7 (1), 145–159. https://doi.org/10.1002/wcc.378.

Rügner, H., Schwientek, M., Milačič, R., Zuliani, T., Vidmar, J., Paunović, M., Laschou, S., Kalogianni, E., Skoulikidis, N., Diamantinie, E., Majone, E., Bellin, A., Chiogna, G., Martinez, E., López de Alda, M., SilviaDíaz-Cruz, M., Grathwohl, P. (2019). Particle bound pollutants in rivers: Results from suspended sediment sampling in Globaqua River Basins. Science of the Total Environment, 647, 645-652. https://doi.org/10.1016/j.scitotenv.2018.08.027

Sedláček, J., Bábek, O., Nováková, T. (2017). Sedimentary record and anthropogenic pollution of a complex, multiple source fed dam reservoirs: An example from the Nové Mlýny reservoir, Czech Republic. Science of the Total Environment, 574, 1456-1471. https://doi.org/10.1016/j.scitotenv.2016.08.127

Simons, D., Richardson, E., Albertson, M., Kodoatie, R. (2004). Geomorphic, hydrologic, hydraulic and sediment transport concepts applied in alluvial rivers. Colorado State Univ. https://www.engr.colostate.edu/~pierre/ce_old/classes/CE716/Geomorphic,%20Hydrologic,%20Hydrau

Stähly, S., Franca, M. J., Robinson, C.T., Schleiss, A.J. (2020). Erosion, transport and deposition of a sediment replenishment under flood conditions. Earth Surface Processes and Landforms, 45(13), 3354-3367. https://doi.org/10.1002/esp.4970

Sundborg, Å. (1992). Lake and reservoir sedimentation prediction and interpretation. Geografiska Annaler: Series A, Physical Geography, 74(2-3), 93-100. https://doi.org/10.1080/04353676.1992.11880353

Szalinska, E., Smolicka, A., Dominik, J. (2013). Discrete and time-integrated sampling for chromium load calculations in a watershed with an impoundment reservoir at an exceptionally low water level. Environmental Science and Pollution Research, 20(6), 4059-4066. 10.1007/s11356-012-1327-9

Szalińska, E., Orlińska-Woźniak, P., Wilk, P. (2020). Sediment load variability in response to climate and land use changes in a Carpathian catchment (Raba River, Poland). Journal of Soils and Sediments, 1-12. https://doi.org/10.1007/s11368-020-02600-8

Szalińska, E., Zemełka, G., Kryłów, M., Orlińska-Woźniak, P., Jakusik, E., Wilk, P. (2021). Climate change impacts on contaminant loads delivered with sediment yields from different land use types in a Carpathian basin. Science of The Total Environment, 755, 142898. https://doi.org/10.1016/j.scitotenv.2020.142898

Szarek-Gwiazda, E., Sadowska, I. (2010). Distribution of grain size and organic matter content in sediments of submontane dam reservoir. Environment Protection Engineering, 36(1), 113-124.

Szlapa, M., Hachaj, P. S. (2017). The impact of processes of sediment transport on storage reservoir functions. Technical Transactions, 114(7), 113-126. https://doi.org/10.4467/2353737XCT.17.112.6653

Szlapa, M., Hachaj, P. S., Krylow, M., Szalinska, E. (2017). Release of nitrogen and phosphorus from bottom sediments of the Dobczyce Reservoir due to dynamic changes in the backwater region. Przemysł Chemiczny, 96(6), 1386–1389. https://doi.org/10.15199/62.2017.6.3

Szlapa, M. (2019). Conditions for creation and change of a dam reservoir backwater region morphodynamics – a case study of Dobczyce Reservoir on the Raba River. (PhD thesis – in Polish)

Thornton, J., Steel, A. and Rast, W. (1996). 'Reservoirs', in Chapman, D. (ed.) Water Quality Assessments - A Guide to Use of Biota, Sediments and Water in Environmental Monitoring. 2nd edn. Cambridge: UNESCO/WHO/UNEP, p. 41.

Wilk, P., Orlińska-Woźniak, P., Gębala, J. (2018a). The river absorption capacity determination as a tool to evaluate state of surface water. Hydrology and Earth System Sciences, 22(2), 1033-1050. https://doi.org/10.5194/hess-22-1033-2018

Wilk, P., Orlińska-Woźniak, P., Gębala, J. (2018b). Mathematical description of a river absorption capacity on the example of the middle Warta catchment. doi:10.5277/epe180407

Wilk, P., Orlińska-Woźniak, P. (2019). Use of the macromodel DNS/SWAT to calculate the natural background of TN and TP in surface waters for the RAC parameter. Architecture Civil Engineering Environment, 12(1). 10.21307/ACEE-2019-017

Wilk-Woźniak, E., Krztoń, W., Górnik, M. (2021). Synergistic impact of socio-economic and climatic changes on the ecosystem of a deep dam reservoir: Case study of the Dobczyce dam reservoir based on a 30-year monitoring study. Science of The Total Environment, 756, 144055. https://doi.org/10.1016/j.scitotenv.2020.144055

Williams, J.R. (1975). Sediment routing for agricultural watersheds 1. JAWRA Journal of the American Water Resources Association, 11(5), 965-974.

Wisser, D., Frolking, S., Hagen, S., Bierkens, M. F. (2013). Beyond peak reservoir storage? A global estimate of declining water storage capacity in large reservoirs. Water Resources Research, 49(9), 5732-5739. https://doi.org/10.1002/wrcr.20452

Wrzesiński, D., Sobkowiak, L. (2020). Transformation of the Flow Regime of a Large Allochthonous River in Central Europe - an Example of the Vistula River in Poland. Water, 12(2), 507. https://doi.org/10.3390/w12020507

Wu, X., Xiang, X., Chen, X., Zhang, X., Hua, W. (2018). Effects of cascade reservoir dams on the streamflow and sediment transport in the Wujiang River basin of the Yangtze River, China. Inland Waters, 8(2), 216-228. https://doi.org/10.1080/20442041.2018.1457850

Wypych, A., Sulikowska, A., Ustrnul, Z., Czekierda, D. (2017). Variability of growing degree days in Poland in response to ongoing climate changes in Europe. International journal of biometeorology, 61(1), 49-59. https://doi.org/10.1007/s00484-016-1190-3

Wypych, A., Ustrnul, Z., Schmatz, D. R. (2018). Long-term variability of air temperature and precipitation conditions in the Polish Carpathians. Journal of Mountain Science, 15(2), 237-253. https://doi.org/10.1007/s11629-017-4374-3

Zarfl, C., Lucía, A. (2018). The connectivity between soil erosion and sediment entrapment in reservoirs. Current Opinion in Environmental Science & Health, 5, 53-59. https://doi.org/10.1016/j.coesh.2018.05.001

Zemełka, G., Kryłów, M., Szalińska van Overdijk, E. (2019). The potential impact of land use changes on heavy metal contamination in the drinking water reservoir catchment (Dobczyce Reservoir, south Poland). Archives of Environmental Protection, 45(2). https://doi.org/10.24425/aep.2019.127975

Zhang, H., Meng, C., Wang, Y., Wang, Y., Li, M. (2020). Comprehensive evaluation of the effects of climate change and land use and land cover change variables on runoff and sediment discharge. Science of The Total Environment, 702, 134401. https://doi.org/10.1016/j.scitotenv.2019.134401

Zhao, G., Mu, X., Jiao, J., Gao, P., Sun, W., Li, E., Wei, Y., Huang, J. (2018). Assessing response of sediment load variation to climate change and human activities with six different approaches. Science of the Total Environment, 639, 773-784. https://doi.org/10.1016/j.scitotenv.2018.05.154

Zhu, H., Bing, H., Wu, Y., Zhou, J., Sun, H., Wang, J., Wang, X. (2019). The spatial and vertical distribution of heavy metal contamination in sediments of the Three Gorges Reservoir determined by anti-seasonal flow regulation. Science of the Total Environment, 664, 79-88. https://doi.org/10.1016/j.scitotenv.2019.02.016

Yang, Y., Bai, L.,Wang, B.,Wu, J., Fu, S., 2019. Reliability of the global climate models during 1961–1999 in arid and semiarid regions of China. Sci. Total Environ. 667, 271–286. https://doi.org/10.1016/j.scitotenv.2019.02.188.

Yen, H., Lu, S., Feng, Q., Wang, R., Gao, J., Brady, D. M., Sharifi, A., Ahn, J., Chen, S., Jeong, J., White, M., Arnold, J. G. (2017). Assessment of optional sediment transport functions via the complex watershed simulation model SWAT. Water, 9(2), 76. https://doi.org/10.3390/w9020076

Vigiak, O., Malagó, A., Bouraoui, F., Vanmaercke, M., Poesen, J. (2015). Adapting SWAT hillslope erosion model to predict sediment concentrations and yields in large basins. Sci. Total Environ. 538, 855–875. https://doi.org/10.1016/j.scitotenv.2015.08.095.

Vercruysse, K., Grabowski, R. C., Rickson, R. J. (2017). Suspended sediment transport dynamics in rivers: Multi-scale drivers of temporal variation. Earth-Science Reviews, 166, 38-52. https://doi.org/10.1016/j.earscirev.2016.12.016

Vörösmarty, C. J., Meybeck, M., Fekete, B., Sharma, K., Green, P., Syvitski, J. P. (2003). Anthropogenic sediment retention: major global impact from registered river impoundments. Global and planetary change, 39(1-2), 169-190. https://doi.org/10.1016/S0921-8181(03)00023-7